Air-Stable Solid-State Photoluminescence Standards for Quantitative Measurements Based on 4′-Phenyl-2,2′:6′,2″-Terpyridine Complexes with Trivalent Lanthanides

Alexander E. Sedykh,[a] Mariia Becker,[b] Marcel T. Seuffert,[a] Dominik Heuler,[a] Moritz Maxeiner,[a] Dirk G. Kurth,[c] Catherine E. Housecroft,[b] Edwin C. Constable,[b] and Klaus Müller-Buschbaum*[a, d]

Correct photoluminescence quantum yield (PLQY) determination in the solid state is vital for numerous application fields, such as photovoltaics, solid lighting or the development of phosphors. In order to increase the limited number of suitable standards for such determinations, two new Ln^{3+}-based complexes with 4′-phenyl-2,2′:6′,2″-terpyridine γ-$[Ln_4(OAc)_{12}(ptpy)_2]$ (**1-Eu** with europium and **1-Tb** with terbium) are presented. The corresponding complexes show solid-state QYs of 58(4) % and 46(3) %, respectively, exhibiting broadband absorption in the UV range from 380–200 nm. As Ln^{3+} ions in general exhibit narrow *f-f* transitions, spectral regions with a broadness of 20–35 nm can be checked. Both complexes have suitable thermal stability, up to 270 °C, and are stable with respect to air and humidity, for **1-Eu** up to 75 % and for **1-Tb** up to 53 % relative humidity. These complexes are altogether suitable as standards to increase the reliability of PLQY determination and proposed to be used for a relative PLQY determination in the solid state.

Introduction

Quantum yield is a crucial experimental value for numerous photoactive materials. Alongside luminescence lifetime, it characterises the overall performance of such materials. By definition, the photoluminescence quantum yield (PLQY or Φ) is the direct ratio of photons emitted to photons absorbed by a substance.[1–3] It can take values between 0 and 1, which can also be presented in percent, between 0 and 100 %. PLQY is an important value to be determined for various materials, such as perovskites,[4–8] carbon-based nanomaterials,[9,10] quantum dots,[5,11,12] and rare-earth element compounds.[13–16] Application areas that require determination of PLQY are numerous, such as photovoltaics,[8,12] LEDs,[5–7] OLEDs,[17–21] bioimaging,[9–11,13,22] and phosphors.[14,23,24] Also for mechanoluminescent materials, PLQY is an important parameter.[25] The number of publications concerning quantum yield rises exponentially.[26]

One of the approaches to determine PLQY is an absolute method that includes direct measurement of the amount of light absorbed and light emitted by the sample, requiring an integration sphere. First, an integrated intensity of the excitation source is determined. Either, an empty integration sphere is measured or a blank sample, for example, a pure solvent without a fluorophore. Second, the integrated intensity of the excitation source is measured when the photoluminescent compound is present in the sphere. From these two measurements, the amount of light absorbed by the material under investigation is determined. Thirdly, the integrated emission intensity of the sample is measured. Finally, a ratio between emitted and absorbed photons is calculated, providing the PLQY. Nevertheless, obtaining a correct quantum yield value is not as straightforward as it might seem. The exact result depends on several factors, including sample preparation and instrumental setup calibration. This includes not only monochromator and detector corrections,[2,27] which are typically provided by the manufacturer, but also a correction of the integration sphere.[2,27] This is especially required in the case of an external integration sphere connected to the instrument *via* optical cables.

[a] *A. E. Sedykh, M. T. Seuffert, D. Heuler, M. Maxeiner, Prof. Dr. K. Müller-Buschbaum*
Institute of Inorganic and Analytical Chemistry
Justus-Liebig-University Giessen
Heinrich-Buff-Ring 17, 35392 Giessen (Germany)
E-mail: kmbac@uni-giessen.de
Homepage: www.uni-giessen.de/fbz/fb08/Inst/iaac/mueller-buschbaum
[b] *Dr. M. Becker, Prof. Dr. C. E. Housecroft, Prof. Dr. E. C. Constable*
Department of Chemistry
University of Basel
BPR 1096, Mattenstrasse 24a
4058 Basel (Switzerland)
[c] *Prof. Dr. D. G. Kurth*
Lehrstuhl für Chemische Technologie der Materialsynthese
Julius-Maximilians-Universität Würzburg
Röntgenring 11
97070 Würzburg (Germany)
[d] *Prof. Dr. K. Müller-Buschbaum*
Center for Materials Research (LAMA)
Justus-Liebig-University Giessen
Heinrich-Buff-Ring 16
35392 Giessen (Germany)

Supporting information for this article is available on the WWW under https://doi.org/10.1002/cptc.202200244

In order to check the instrumental setup for PLQY measurements, it is necessary to measure several photoluminescence standards. Most of the standards proposed in the literature are solutions of fluorophores, such as quinine hydrogen sulfate,[28–30] fluorescein,[29–32] and sulforhodamine 101.[30,31,33] There are fewer solid-state photoluminescence standards available, with sodium salicylate being most reported regarding its quantitative photoluminescence properties.[3,26,34] This provides a certain problem for solid-state spectroscopy: despite photoactive compounds typically being used in the solid-state in most applications, a larger number of PLQY standards are investigated in solutions at concentrations 10^{-6} to 10^{-4} M.[28–33] Furthermore, there is a tendency in publications, to neither describe the instrumental setup in detail for PLQY determination nor specify if the setup was checked with photoluminescence standards.

In addition, samples exhibiting fluorescence can have photon reabsorption, affecting the observed PLQY. This is especially the case for samples in solution, for which the observed quantum yield depends on the fluorophore concentration.[28,29] Furthermore, sample concentration can also influence emission and excitation profiles and their maxima.[29] For solid-state samples, particle size can affect reflectance and transmission of photons, which also potentially influence the observed PLQY. Simple blue range fluorophores, for example, pyrene or anthracene, despite being available and very stable, are not suitable to be used as common photoluminescence standards. Their photoluminescence properties, especially PLQY, are dependent on chemical impurities, structural defects, and crystallite size.[35,36] The difference in the absolute quantum yield for the same compound can be as high as three times for a nominally identical purity grade.[35] For solid-state phosphors with dopants, such as $BaMgAl_{10}O_{17}:Eu^{2+}$, PLQY depends on the excitation wavelength, particle size and its distribution, temperature, and dopant concentration.[26]

Trivalent lanthanide coordination compounds typically have a ligand-based excitation in the UV followed by *4f–4f* emission in the visible/NIR range.[14,37] This eliminates possible photon reabsorption since the shift between excitation and emission is several hundred nanometres. Typically, the most intense Ln^{3+} emitters in the visible range are Tb^{3+} with green emission colour and Eu^{3+} with red emission colour. However, for trivalent lanthanide compounds reported by various researchers, there are differences in the data presented. One such example is the trivalent europium complex [Eu(tta)$_3$(phen)] (tta = 4,4,4-trifluoro-1-(2-thienyl)-1,3-butanedione, phen = phenanthroline), its quantitative photoluminescence properties being reported in several publications.[38–46] The difference in the reported absolute quantum yields for this complex in the solid-state ranges from 30 to 85 %.[38–42] It is not possible to determine unambiguously what influences the photoluminescence properties of this complex. Possibly, they depend on sample preparation and/or synthesis, even when the latter was performed according to the same literature method.[38,40,44–47] Moreover, also the observed lifetimes reported for [Eu(tta)$_3$(phen)] differ from 0.67 to 0.98 ms.[40–46] The overall emission intensity decay time is another important quantitative photoluminescence value. In comparison to PLQY measurements, overall emission decay analysis is more reliable in terms of the trustworthiness of the results. As the emission decay is fitted, the goodness-of-fit and amount of exponential decay components indicate data quality. Thus, the difference in the reported PL lifetime for [Eu(tta)$_3$(phen)] indicates its limited suitability as a PL standard.

Having a well-reported PLQY value for photoluminescence compounds is of importance for calculating quantum yields relative to a reference material. For this reason, excitation and emission regions of both compounds, newly reported and the reference one, at best, should be as close to one another as possible.[27] This can be well implemented for trivalent lanthanide phosphors since Ln^{3+} energy levels and therefore *4f–4f* emission transition positions are almost independent of the chemical surroundings.[48]

4′-Phenyl-2,2′:6′,2″-terpyridine (ptpy) was chosen as a ligand for Ln^{3+} for achieving new suitable solid-state photoluminescence standards. 2,2′:6′,2″-terpyridine derivatives are excellent sensitiser ligands for trivalent lanthanides, especially for Eu^{3+}, for which coordination compounds show quantum yields >50 %.[49–55] Because for higher PLQY values, the error coming from improper measurements is easier to observe, it is important to have a PL standard with a high quantum yield. Moreover, trivalent lanthanide metal coordination compounds with 2,2′:6′,2″-terpyridines have a broad excitation range up to 380 nm.[49–54] 4′-Phenyl-2,2′:6′,2″-terpyridine is one of the simplest terpyridine derivatives and can be easily synthesised "one-pot" on a gram scale within several hours.[56] One potential drawback can be air and moisture sensitivity of trivalent lanthanide coordination compounds, especially with N-donor ligands.[57–59] Also, typically, for coordination compounds of Tb^{3+} with 2,2′:6′,2″-terpyridines, the quantum yield is several times lower than for Eu^{3+} analogues[49,50,52] due to the position of the ligand triplet state energy level.[60,61] This renders Tb^{3+} complexes with 2,2′:6′,2″-terpyridines potentially less suitable for the use as photoluminescence standards. However, both points can be overcome, if a suitable coordination environment and crystal system are obtained, as we show in this manuscript. As a result of screening trivalent lanthanide coordination compounds with ptpy, two isostructural tetrameric complexes were found to be very satisfactory for the use as solid-state trivalent lanthanide-based photoluminescence standards: γ-[$Eu_4(OAc)_{12}(ptpy)_2$] (**1-Eu**) and γ-[$Tb_4(OAc)_{12}(ptpy)_2$] (**1-Tb**). Both compounds show high quantum yields, namely 58(4) % for **1-Eu** and 46(3) % for **1-Tb**, and show air and thermal stability.

Results and Discussion

The tetrameric complexes γ-[$Eu_4(OAc)_{12}(ptpy)_2$] (**1-Eu**) and γ-[$Tb_4(OAc)_{12}(ptpy)_2$] (**1-Tb**) show qualitatively typical photophysical properties for trivalent lanthanide compounds with an efficient sensitiser ligand. Both, **1-Eu** and **1-Tb**, have a broad organic ligand-based excitation in the UV region up to 370 nm ($S_n \leftarrow S_0$, labelled in light blue in Figure 1). The direct *4f–4f* excitation bands are of low intensity (labelled in violet in

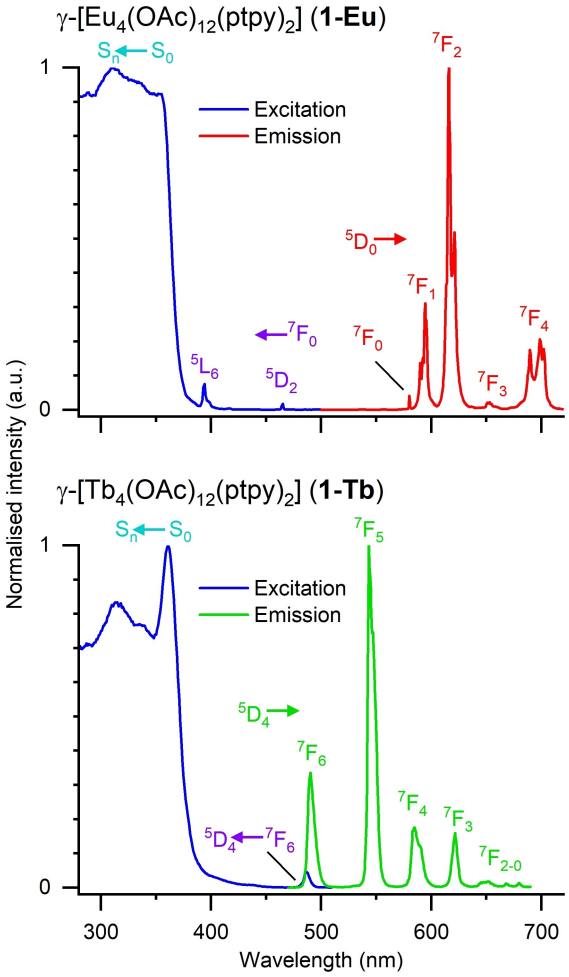

Figure 1. Normalised solid-state room temperature excitation (blue, λ_{em} = 616 nm for **1-Eu** and 585 nm for **1-Tb**) and emission spectra (red for **1-Eu** and green for **1-Tb**, λ_{ex} = 350 nm) of γ-$[Eu_4(OAc)_{12}(ptpy)_2]$ (**1-Eu**, top) and γ-$[Tb_4(OAc)_{12}(ptpy)_2]$ (**1-Tb**, bottom).

Figure 1). Following excitation and an energy transfer from the ligand system to a metal ion, emission takes place with characteristic narrow *4f–4f* transitions for Eu^{3+} ($^5D_0 \rightarrow {}^7F_J$, J = 0-6) and Tb^{3+} ($^5D_4 \rightarrow {}^7F_J$, J = 6-0) (Figure 1). However, the transitions $^5D_0 \rightarrow {}^7F_5$ and $^5D_0 \rightarrow {}^7F_6$ of trivalent europium in the compounds obtained are of very low intensity, as can be seen in additional spectra in the SI (Figures S1-S3). Due to the spectral range limitations of the setups used and the low intensities of these transitions, they were not included in the PLQY determination. Enlarged spectra of trivalent terbium compounds obtained are also presented in the SI (Figures S4-S6).

For the tetrameric complex **1-Eu**, the presence of two Eu^{3+} emissive centres can be observed for the transition $^5D_0 \rightarrow {}^7F_0$ (Figure 2), as both states are non-degenerative. Assignment of both bands to crystallographic sites could be done with the empirical linear relationship (Equation 1):[62]

$$\tilde{\nu}_{calc}^{0\rightarrow0} = \tilde{\nu}_{free}^{0\rightarrow0} + C_{CN}\sum_{i}^{CN} n_i\delta_i \qquad (1)$$

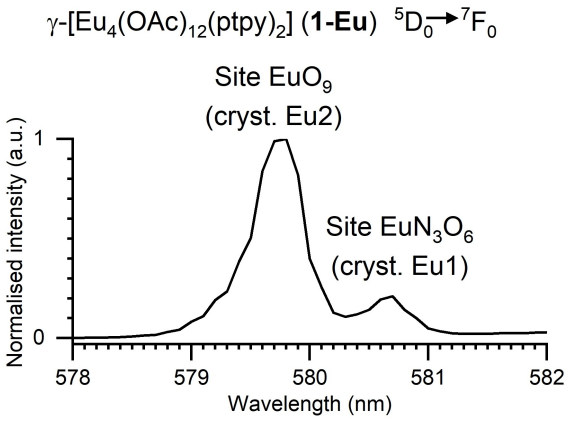

Figure 2. Normalised solid-state room temperature high-resolution (step 0.1 nm, slit 0.1 nm) emission spectrum (λ_{ex} = 350 nm) of γ-$[Eu_4(OAc)_{12}(ptpy)_2]$ (**1-Eu**) $^5D_0 \rightarrow {}^7F_0$ transition indicating the presence of two emissive Eu^{3+} centres (crystallographic site Eu1 refers to EuN_3O_6, crystallographic site Eu2 to EuO_9).

Thereby, the expected energy ($\tilde{\nu}_{calc}^{0\rightarrow0}$) of the $^5D_0 \rightarrow {}^7F_0$ transition can be calculated from the free ion transition energy $\tilde{\nu}_{free}^{0\rightarrow0}$ (17374 cm^{-1})[62] and the sum of experimental nephelauxetic parameters: $\delta_{O\text{-acetate}} = -15.5$ cm^{-1}[63] and $\delta_{N\text{-pyridine}} = -25.3$ cm^{-1}.[64] The coordination number correction factor C_{CN} is equal to 1 in the case of a CN of nine.[62] For two Eu^{3+} sites in **1-Eu**, the calculated energies for $^5D_0 \rightarrow {}^7F_0$ are 17235 cm^{-1} for EuO_9 (crystallographic site Eu2 coordinated only by acetates, observed 17247 cm^{-1}) and 17205 cm^{-1} for EuN_3O_6 (crystallographic site Eu1 coordinated by terpyridine and acetates, observed 17221 cm^{-1}).

The quantitative photophysical properties of γ-$[Ln_4(OAc)_{12}(ptpy)_2]$ (**1-Eu** and **1-Tb**) were investigated thoroughly, varying the measurement parameters. For overall emission decay time determinations, both, the excitation and emission wavelengths were varied. Photoluminescence lifetimes of **1-Ln** are independent of the measurement parameters, being 1.71(5) ms for **1-Eu** and 1.05(2) ms for **1-Tb**. Despite the presence of two possible Ln^{3+} emission centres, every single decay could be fitted with a monoexponential function, with a lifetime value being independent from the emission wavelength. A summary of the photophysical properties of **1-Ln** is presented in Table 1, together with more details provided in the SI (Tables S1–S5).

In order to exclude potential instrumental errors, quantum yields of both, **1-Eu** and **1-Tb**, were independently investigated and measured on two setups of different manufacturers. In summary, Setup I consists of a HORIBA Fluorolog 3 spectrophotometer equipped with an external integrating sphere, and square-based micro cell quartz cuvettes (Figure 3, top). Setup II is constituted by a Hamamatsu C11347 Quantaurus-QY, an instrument dedicated to quantum yield determinations, in which round quartz dishes with lids are used as cuvettes (Figure 3, bottom). For both setups, the overall quantum yield values are consistent within the error ranges, 57.9(3.9)/61.8(1) % for **1-Eu** and 45.8(2.3)/45.5(7) % for **1-Tb** (Table 1). Since trivalent lanthanides have narrow individual *f-f* transitions, also

Table 1. Quantitative photoluminescence data for **1-Eu** and **1-Tb**: Overall emission decay time, overall quantum yield, individual *4f–4f* transitions quantum yield.

Compound/*4f–4f* transition	τ_{Ln} [a] [ms]	Setup I Φ_{obs} [a,b] [%]	Setup II Φ_{obs} [c] [%]
γ-$[Eu_4(OAc)_{12}(ptpy)_2]$ (**1-Eu**)	1.71(5)	57.9(3.9)[d]	61.8(1)[d]
$^5D_0 \rightarrow {}^7F_1$ (583–605 nm)		8.5(7)	9.1(1)
$^5D_0 \rightarrow {}^7F_2$ (605–635 nm)		32.8(2.2)	33.4(1)
$^5D_0 \rightarrow {}^7F_4$ (670–715 nm)		14.8(1.1)	17.1(1)
γ-$[Tb_4(OAc)_{12}(ptpy)_2]$ (**1-Tb**)	1.05(2)	45.8(2.3)[e]	45.5(7)[e]
$^5D_4 \rightarrow {}^7F_6$ (475-515 nm)		8.3(4)	8.2(2)
$^5D_4 \rightarrow {}^7F_5$ (530–565 nm)		25.5(1.3)	25.3(4)
$^5D_4 \rightarrow {}^7F_4$ (570–605 nm)		6.4(4)	6.3(1)
$^5D_4 \rightarrow {}^7F_3$ (610–635 nm)		3.9(3)	3.8(1)

[a] Summary of multiple determinations with different measurement parameters, including λ_{ex} variation, see the Supporting Information for detailed data. [b] MgO was used as reference material for QY determinations. [c] λ_{ex} = 350 nm. [d] λ_{em} = 575–720 nm. [e] λ_{em} = 475–690 nm.

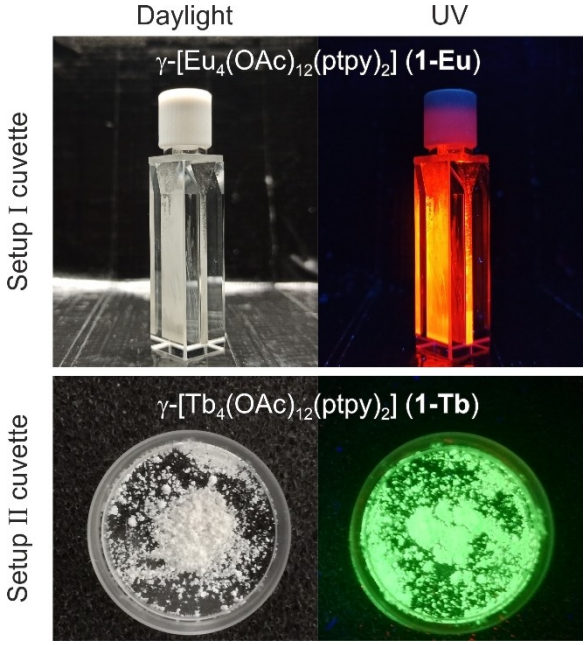

Figure 3. Difference between the cuvettes used for both QY measurement setups. Top: square-based micro cell quartz cuvette (Setup I) with **1-Eu** (as a powder smeared on the cuvette walls) under daylight and a UV lamp. Bottom: Round quartz dish cuvette (Setup II) with **1-Tb** (as a powder filled in the cuvette) under daylight and a UV lamp.

quantum yield values for the spectral regions (broadness 20–35 nm) of the most intense transitions were evaluated (Table 1). They are identical for both setups, except for the $^5D_0 \rightarrow {}^7F_4$ transition in the far-red region 670–715 nm. This indicates a minor difference in the instrumental setup correction for this region. Analysis of QY values for narrow spectral regions can help with troubleshooting by instrumental setup calibration and checking.

As mentioned before, absolute PLQY measurements are not a trivial matter, e.g., for solid-state samples. For example, for setup I, generation of a proper correction is required since an external integration sphere is used. Before the QY measurements, both setups were checked by several typical photoluminescence standards (see SI Table S6). For the typical solid-state photoluminescence standard sodium salicylate (λ_{ex} 340 nm, λ_{em} 365–600 nm), the observed PLQY for both setups – 53.4(2.0) % and 54.6(2) % – are in the data range presented in the literature of 53–57 %..[3,34] For quinine hydrogen sulfate at several concentrations (λ_{ex} 350 nm, λ_{em} 380–660 nm, 10^{-3}–10^{-5} M), the observed PLQY values determined on both setups are similar to the literature.[28,29] For anthracene (λ_{ex} 340 nm, λ_{em} 365–500 nm, 10^{-3}–10^{-5} M), the observed QY measured on both setups is lower at all concentrations by one-fourth of the absolute value reported in the literature.[29] Since these three compounds presented in the literature have close excitation and emission regions, the difference in the data shows that also for a QY measurement in solution, caution is required. This again indicates the necessity to have a suitable set of photoluminescence standards for QY measurements.

UV-Vis reflectance spectra are necessary for relative quantum yield determination.[65] Accordingly, for both, **1-Eu** and **1-Tb**, reflectance spectra were also recorded. Both compounds exhibit a broad organic-based absorption in the UV from 360 up to at least 200 nm. Spectra are provided in the SI in graphical form (SI Figure S7) as well as a table for the ligand-based absorption (SI Table S8).

The thermal stability of the tetrameric complexes **1-Ln** was investigated by simultaneous thermal analysis (STA). Both compounds have reasonable thermal stability, incongruently melting at 280 °C for **1-Eu** and 270 °C for **1-Tb** (Figure 4). Shortly after the melting point, the melt formed becomes volatile and the organic component decomposes oxidatively.

In addition to thermal stability, sensitivity to humidity was tested for the complexes **1-Ln**, since lanthanide compounds with N-donor ligands are prone to hydration.[57–59] The europium containing complex **1-Eu** was stable at 75 % relative humidity for a week, showing no changes in PXRD nor in the photoluminescence properties. Its terbium analogue **1-Tb** is slightly less stable, up to 53 % relative humidity for a week. At 75 % relative humidity, **1-Tb** slowly hydrolyses, showing changes in PXRD and a slight decrease of overall emission decay time and QY. Both complexes γ-$[Ln_4(OAc)_{12}(ptpy)_2]$ (**1-Ln**) can be considered stable in air, against humidity, and are thermally stable.

For suitability as potential photophysical standards, it is of importance to deliberately investigate and standardise the synthesis conditions of the potential standards, because the product purity can strongly influence the quantitative photophysical properties. Therefore, for **1-Ln**, we deliberately clarified the synthesis conditions and possible side products including all formation conditions. In the reaction between europium or terbium acetate hydrate with ptpy, several possible compounds can in principle be formed (see Scheme 1). Conversion of the starting materials and selectivity of the synthesis depends on the reaction conditions, especially on the water concentration and reaction temperature. All possible products are linear tetrameric complexes with a similar core structure, though with different crystal packing. The tetrameric complex hydrate $[Eu_4(OAc)_{12}(ptpy)_2]\cdot 2H_2O$ (**2-Eu**) was obtained if water was

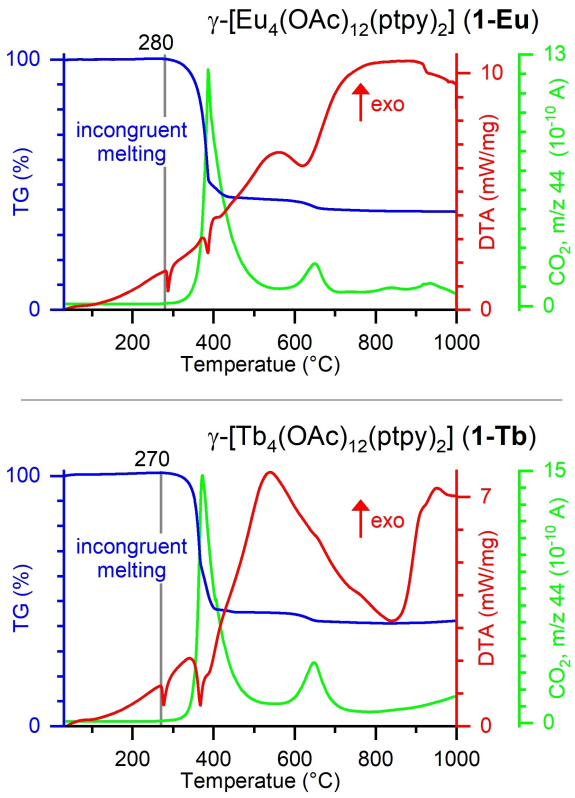

Figure 4. Thermal analysis of γ-$[Eu_4(OAc)_{12}(ptpy)_2]$ (**1-Eu**) and γ-$[Tb_4(OAc)_{12}(ptpy)_2]$ (**1-Tb**) by simultaneous TG/DTA/MS. The heat-flow (DTA) is depicted in red, the mass loss (TG) in blue, MS ion current of m/z 44 (CO_2) in green. Measured in an oxidative atmosphere (synthetic air) with a heating rate of 5 K·min^{-1}.

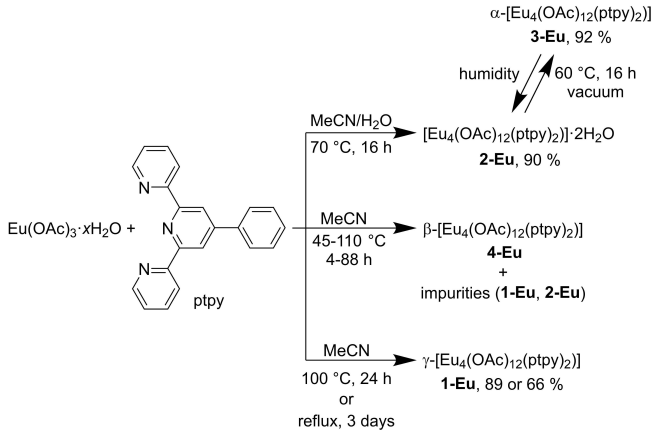

Scheme 1. Deliberate determination of synthesis conditions of the standard **1-Eu** and of potential side products **2-Eu**, **3-Eu** and **4-Eu**.

deliberately added to the reaction (Scheme 1, top). Product **2-Eu** can be dehydrated under the formation of α-$[Eu_4(OAc)_{12}(ptpy)_2]$ (**3-Eu**), the reaction being reversible (Scheme 1, top right). For β-$[Eu_4(OAc)_{12}(ptpy)_2]$ (**4-Eu**), no suitable reaction conditions were found to obtain it phase pure as a bulk material (Scheme 1, middle). γ-$[Eu_4(OAc)_{12}(ptpy)_2]$ (**1-Eu**) was obtained at high temperatures with longer reaction times (Scheme 1, bottom). Similar reactivity was observed for terbium, with **1-Tb**, **2-Tb**, and **3-Tb** obtained phase pure. For both, **1-Eu** and **1-Tb**, several synthetic approaches were investigated, three variants being presented, since these phases are the most suitable candidates to be used as solid-state photoluminescence standards (see SI, Bulk material syntheses). Altogether, the synthesis conditions have been deliberately clarified including possible side phases. Thereby, potential errors by other products and impurities were prevented, so that the problem of synthesis conditions and their influence on photophysical data, such as QY, can be ruled out for the proposed standards.

Products **1**–**4** have a similar tetrameric molecular structure of $[Ln_4(OAc)_{12}(ptpy)_2]$ (Ln = Eu, Tb; Figure 5). For all, there is an inversion point between the two metal ions in the centre of the complex. The ligand ptpy is coordinated to the outer lanthanide ions and connected to one of the centre lanthanide ions through three acetate anions. For two of them, one oxygen atom is coordinated to both lanthanide ions. Two central lanthanide ions are connected *via* two acetate anions, again, with two oxygen atoms being coordinated to both metal centres. Despite having a different coordination environment, each of the lanthanide ions has a distorted capped square antiprismatic coordination environment (CN 9). Analogous linear tetrameric structures are known for Ln^{3+}.[66–71] The closest examples are complexes, such as $[Eu_4(diHal\text{-}benz)_{12}(terpy)_2]$, with 2,2′:6′,2″-terpyridine and 3,5-dihalobenzoates.[67,68] For these complexes, two types of coordination spheres are reported: with CN 8 for Eu^{3+} and a distorted square antiprism and a bicapped trigonal prismatic coordination polyhedra,[67] or two different CNs of 7 for inner metal centres (capped octahedral coordination polyhedra) and 8 for outer ones (bicapped trigonal prismatic coordination polyhedra).[68] The complex $[Eu_4(OAc)_{12}Cu_2L_2]\cdot 2H_2O$ with acetate ligands has a molecular structure similar to compounds **1**–**4**, with CuL (L = N,N′-bis(3-methoxysalicylidene)butane-1,4-diamine) occupying capping position analogous to ptpy in **1**–**4**.[66] In this complex, all trivalent europium ions have a CN of 9 and capped square antiprismatic coordination environment,[66] showing the closest relation to **1**–**4**, reported here. Also, Eu^{3+} tetrameric complexes are known with 1,10-phenanthroline and benzoate derivatives, of a general formula $[Eu_4(benz)_m(phen)_n]\cdot xH_2O$ (m = 6 or 10, n = 4 or 6, x = 0–12).[69–71] In these complexes, a typical coordination number for Eu^{3+} is 8, exhibiting square antiprismatic coordination polyhedra,[69–71] while in one example inner metal ions have CN of 9 with a capped square antiprismatic coordination environment.[71]

Interatomic distances between trivalent europium centres for **1-Eu**, **3-Eu**, and **4-Eu** are well comparable and vary between 405.26(7) and 415.19(4) pm. These are analogous to interatomic distances in similar tetrameric structures of trivalent europium, which are in the range of 398.45–452.05 pm[66–68,71] The interatomic distances Eu–N for **1-Eu**, **3-Eu**, and **4-Eu** lie in the range of 255.7(2)-260.0(4) pm (literature 253.1–263.9 pm).[66–71] Eu–O interatomic distances for these compounds are in the range of 231.6(4)-267.2(3) pm (literature 220.4–280.0 pm).[66–71] Details on the crystallographic data, including coordination

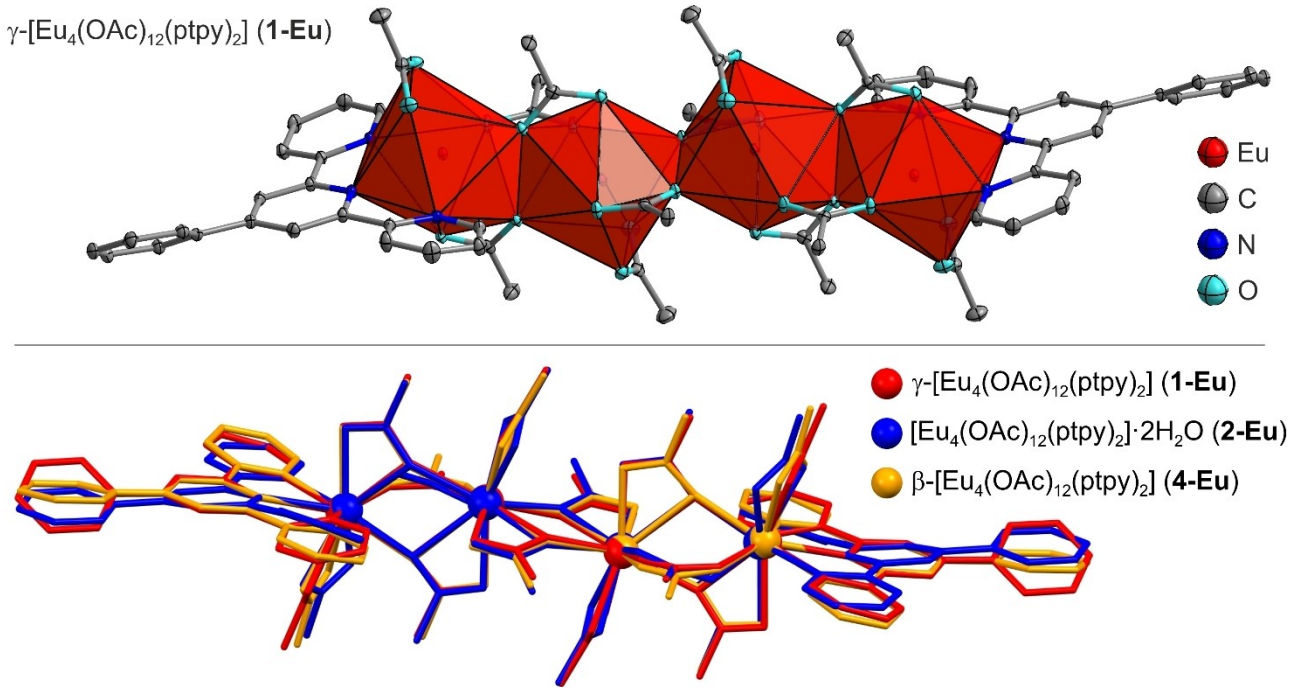

Figure 5. Top: X-ray crystal structure of a complex unit of γ-$[Eu_4(OAc)_{12}(ptpy)_2]$ (**1-Eu**). Thermal ellipsoids depict a 50% probability level of the atoms (Eu red, C grey, N blue, O light blue, hydrogen atoms are omitted). Bottom: A structural overlay as wireframe model of γ-$[Eu_4(OAc)_{12}(ptpy)_2]$ (**1-Eu**, red), $[Eu_4(OAc)_{12}(ptpy)_2]\cdot 2H_2O$ (**2-Eu**, blue), and β-$[Eu_4(OAc)_{12}(ptpy)_2]$ (**4-Eu**, orange); all structures presented were measured at 100 K.

sphere interatomic distances and angles, for **1**–**4** obtained can be found in the SI (Tables S9-S11).

Photophysical and thermal properties of the complexes **2-Ln** and **3-Ln** were also investigated. They show qualitatively typical photophysical properties for trivalent lanthanide coordination compounds (spectra are presented in the SI, Figures S2, S3, S5, and S6). PLQY's and overall emission intensity decay times of these Eu^{3+} tetrameric complexes are 58.6(7) %/1.720(2) ms for **2-Eu** and 61.9(1.2) %/1.804(2) ms for **3-Eu**. For their Tb^{3+} analogues, they are 28.9(5) %/0.7077(6) ms for **2-Tb** and 23.0(4) %/0.4122(5) ms for **3-Tb**, noticeably lower than for **1-Tb**. The observed lifetimes and quantum yields of the complexes obtained are well comparable to trivalent europium and terbium coordination compounds with efficient sensitiser ligands,[57,72–76] especially with 2,2′:6′,2″-terpyridine derivatives.[50,52,55,67] Simultaneous thermal analyses of **2-Ln** and **3-Ln** are presented in the SI (Figures S17-S20). To summarise, complexes **2-Ln** release incorporated water above 100 °C. The resulting complexes **3-Eu** and **3-Tb** incongruently melt at 215 and 200 °C, respectively, which is 70 °C lower than for **1-Ln**. Therefore, it is possible to check the purity of compounds obtained e.g., by a melting point determination. After incongruent melting, **1-Ln** and **3-Ln** have similar thermal properties: at 335–350 °C the organic part becomes volatile and decomposes, resulting in the formation of corresponding lanthanide oxycarbonate, which decomposes upon further heating to the oxide (Eu_2O_3 or Tb_4O_7).

Conclusion

Two new complexes γ-$[Eu_4(OAc)_{12}(ptpy)_2]$ (**1-Eu**) and γ-$[Tb_4(OAc)_{12}(ptpy)_2]$ (**1-Tb**) were synthesised and considered suitable to be used as photoluminescence solid-state standards for the determination of quantum yields. These two complexes show high quantum yields of 58(4) % and 46(3) % for **1-Eu** and **1-Tb**, respectively, with the absolute PLQY being determined on two independent instrumental setups in different scientific groups. The two new PLQY standards are thermally stable, incongruently melting at 280 °C (**1-Eu**) and 270 °C (**1-Tb**), stable on air, and show good insensitivity against humidity. The syntheses conditions of both compounds were deliberately investigated also regarding the formation of potential side products. This allows for providing suitable synthesis conditions in order to prevent unwanted influences of synthesis conditions on the quantum yield. In summary, the new complexes can be used as reference materials for a relative determination of photoluminescence quantum yields in the solid-state, especially for coordination compounds containing trivalent europium or terbium. Importantly, both, calibration and checking of the instrumental setup for measuring absolute PLQY's (spectrophotometer with an integration sphere) using both complexes γ-$[Ln_4(OAc)_{12}(ptpy)_2]$ (**1-Ln**) can increase the quality of the reported data not only for trivalent lanthanide oriented scientists, but also chemists of other fields working with photoactive solid-state compounds.

Experimental Section

Deliberate synthesis and detailed analytical data of all products can be found in the SI. $Eu(OAc)_3{\cdot}xH_2O$, $Tb(OAc)_3{\cdot}xH_2O$, and solvents (> 99%) were used as received. 4′-phenyl-2,2′:6′,2″-terpyridine was synthesised from 2-acetylpyridine and benzaldehyde as described in the literature.[56] The vacuum line, Duran® culture tubes (12× 100 mm, test tubes with a screw cap), Duran® glass ampoules (outer ø 10 mm, wall thickness 1.5 mm), and special quick-fits for their connection to the vacuum line were used for the synthesis. Products were stored and prepared for analysis on air unless otherwise stated. For humidity stability tests, saturated solutions of $Mg(NO_3)_2{\cdot}6H_2O$ (53% relative humidity at 25 °C) and NaCl (75% relative humidity at 25 °C) in deionised water were prepared; samples were stored together with a saturated solution in a desiccator.

Deposition Numbers 2163397 (for **1-Eu** at 300 K), 2163398 (for **1-Eu** at 100 K), 2163399 (for **2-Eu**), 2164887 (for **3-Eu**), 2164888 (for **3-Tb**), 2163400 (for **4-Eu**) contain the supplementary crystallographic data for this paper. These data are provided free of charge by the joint Cambridge Crystallographic Data Centre and Fachinformationszentrum Karlsruhe Access Structures service.

The Supporting Information (26 pages) contains details on bulk material and single crystal syntheses, photoluminescence spectra, tables with quantitative photoluminescence data, tables with crystallographic data, tables with selected interatomic distances and angles, powder X-ray diffraction plots, and simultaneous thermal analysis plots.

Photoluminescence Investigations. Excitation and emission spectra were recorded in the front-face geometry using the FluoroEssence software on a Fluorolog 3 spectrometer (HORIBA) equipped with a dual lamp house, Xe short-arc lamp (USHIO, 450 W), Xe short-arc flashlamp (Exelitas FX-1102, average power 10 W), double-grated monochromators, a photomultiplier detector (R928P), and a TCSPC upgrade. Excitation and emission spectra were corrected for the spectral response of monochromators and detector using correction files provided by the manufacturer. Excitation spectra were additionally corrected for the spectral distribution of the lamp by the use of the reference photodiode detector. To avoid the second-order light reflection by monochromators, a long-pass filter (Newport, cut-off wavelength 495 nm) was used. Overall emission decay times were measured using the DataStation software. The microsecond flash-lamp was used for the excitation. Exponential tail fitting was used for the calculation of lifetimes with the mono-exponential decay function $I(t) = A + B \cdot e^{(-t/\tau)}$ using the Decay Analysis Software 6. The fit quality was confirmed by χ^2 values.

For the quantum yield determinations performed at the Justus-Liebig-University Giessen (setup I), a second Fluorolog 3 (HORIBA) was used, equipped with a Xe short-arc lamp (USHIO, 450 W), double-grated monochromators, a photomultiplier detector (R928P), and a Quanta-Phi Integrating Sphere (HORIBA). For measurements of solid samples, the latter were filled in a micro cell quartz cuvette (Starna 18-F/ST/C/Q/10; fluorescence with ST/C closed-cap, material UV quartz glass Spectrosil Q, pathlength 10 mm, matched); magnesium oxide was used as reference material. The sample was measured several times and the average quantum yield with a standard deviation was calculated from these measurements. Therefore, given standard deviations represent the measurement error, the actual error of the method can be as high as 20% of the given quantum yield value.

For the quantum yield determinations performed at the University of Basel (setup II), an absolute photoluminescence quantum yield spectrometer C11347 Quantaurus-QY (Hamamatsu) was used. Typical fluorescence quartz cuvettes with a square base and 10 mm pathlength were used for the measurements in solution. Milli-Q water and HPLC grade ethanol were used for solutions preparation. The laboratory dishes with caps both made of synthetic quartz were used as cuvettes for powder measurements, with the solid sample being put in the middle of the cuvette. For γ-$[Tb_4(OAc)_{12}(ptpy)_2]$ (**1-Tb**) complex, the powder was milled with a help of a mortar and pestle prior to the measurement. PLQY was recorded (in solution and powder) five times for each compound with a slight rotation of the sample between the measurements.

Each setup for quantum yield measurements was counter-checked by measuring several standards (solutions with various concentrations of anthracene, quinine hydrogen sulfate, fluorescein, and sulforhodamine 101[28–33] and sodium salicylate as a solid,[3,34] see SI Table S6).

UV-Vis Spectroscopy. Reflectance spectroscopy data has been acquired with a Cary 5000 Series UV-VIS-NIR Spectrophotometer (Agilent Technologies) equipped with a diffuse reflectance accessory Praying Mantis™ (Harrick Scientific Products) and used in double-beam mode with full slit height. Powdered polytetrafluoroethylene (Sigma-Aldrich, 1 μm particle size) was used as reference material. The source changeover from a tungsten-halogen VIS-lamp to a deuterium-arc UV-lamp was done at 270 nm (for **1-Eu**) or 370 nm (for **1-Tb**) to avoid interferences with the absorption peak of the ligand. The spectral bandwidth was set to 5 nm to achieve a higher signal intensity. Both, the reference and the sample were ground, filled into the sample cups, and levelled to get a flattened surface. For both, the reference and the sample, the signal was maximised by focusing the beam onto the powder surface. First, a background correction spectrum was recorded. Then, a spectrum with uncorrected reflectance was recorded with the reflectance set to 100% at 700 nm. The sample spectrum was corrected with the instrument software (Cary WinUV) by the mathematical operation $\%R^{\text{sample}}{}_{\text{corr}} = \%R^{\text{sample}}/\%R^{\text{reference}}$.

Single Crystal X-ray Diffraction Analysis. **Single** crystals of the products were mounted on a goniometer head using a perfluorinated ether for measurements at 100 K or a silicon grease for measurements at 300 K. Data collection was performed using Mo–Kα_1 X-ray radiation with a BRUKER AXS D8 VENTURE (for **1-Eu** at 100 and 300 K, for **2-Eu** and **4-Eu** at 100 K) using the BRUKER AXS Apex software package.[77] Data processing was accomplished with XPREP.[78] A structure solution was carried out with direct methods using SHELXT[79] and the obtained crystal structure was refined with least square techniques using SHELXL[80] on the graphical platform shelXle.[81]

Powder X-ray Diffraction Analysis. Inside a glovebox, a sample was filled in a glass mark tube (Ø 0.3 mm, Hilgenberg GmbH), which was cut and sealed with a picein wax. Diffraction data were collected in a Debye-Scherrer (transmission) geometry with a powder X-ray diffractometer STOE Stadi P equipped with a focusing Ge(111) monochromator and a MYTHEN 1 K strip detector (angular range 12.5° in 2θ) using Cu–Kα_1 X-ray radiation. The data collection was done in a 2θ range of 2–60° with a step size of 0.015° and an integration time of 20 s. Baseline correction was performed using the BRUKER AXS Diffrac.Eva software.

For the Rietveld refinement, data collection was done with the above-mentioned X-ray diffractometer STOE Stadi P in a 2θ range of 3–90°. Three runs with a step size of 0.015° and an offset of 0.005° and an integration time of 60 s were measured and merged (effective stepsize of 0.005°). Rietveld refinement was done with a BRUKER AXS Topas-Academic 7 software.[82] For the Rietveld structure refinement of **3-Ln**, the X-ray single crystal structure of **2-Eu** was used as a starting model: water molecule was omitted,

each acetate group and each ligand ring were treated as a rigid body.

After the humidity stability tests, the samples were measured in Bragg-Brentano (reflection) geometry on a powder X-ray diffractometer PANalytical X'Pert Pro equipped with a X'Celerator detector using Cu-K_α X-ray radiation. Data collection was done in a 2θ range of 5–60° with a step size of 0.0167° and an integration time of 120 s.

Thermal Analysis. Simultaneous thermogravimetry and differential thermal analysis were performed using a NETZSCH STA-409-PC coupled with a QMS 403 Aëolos Quadro. Argon (20 mL·min^{-1}) was used as protective gas; synthetic air (30 mL·min^{-1}) was used as working gas. Samples (10–20 mg) were heated up to 1000 °C with a heating rate of 5 °C·min^{-1}. Melting character (for **1-Eu**, **1-Tb**, **3-Eu**, and **3-Tb**) was determined using melting point meter Krüss KSP1 N.

CHN Analysis. For CHN analysis, the compounds were placed in a tin crucible with approximately one mass equivalent of V_2O_5 (oxidation catalyst). Analyses were done with a Thermo FlashEA 1112 Series.

Acknowledgements

The authors gratefully acknowledge the Deutsche Forschungsgemeinschaft for supporting this work within the project MU-1562/13-1, the Justus-Liebig University Giessen for a knock-on financing and general support, and the University of Basel for general support. The authors acknowledge Stephanie Maaß (Julius-Maximilians-University of Würzburg) for the synthesis of 4′-phenyl-2,2′:6′,2″-terpyridine. Open Access funding enabled and organized by Projekt DEAL.

Conflict of Interest

The authors declare no conflict of interest.

Data Availability Statement

The data that support the findings of this study are available in the supplementary material of this article.

Keywords: analytical methods · lanthanides · photovoltaics · quantum yields · solid state

[1] G. A. Crosby, J. N. Demas, *J. Phys. Chem.* **1971**, *75*, 991–1024.
[2] F. Fries, S. Reineke, *Sci. Rep.* **2019**, *9*, 15638.
[3] M. S. Wrighton, D. S. Ginley, D. L. Morse, *J. Phys. Chem.* **1974**, *78*, 2229–2233.
[4] M. Bidikoudi, E. Fresta, R. D. Costa, *Chem. Commun.* **2018**, *54*, 8150–8169.
[5] R. Shwetharani, V. Nayak, M. S. Jyothi, R. Geetha Balakrishna, *J. Alloys Compd.* **2020**, *834*, 155246.
[6] E. V. Ushakova, S. A. Cherevkov, V. A. Kuznetsova, A. V. Baranov, *Materials* **2019**, *12*, 3845.
[7] G. K. Grandhi, H. J. Kim, N. S. M. Viswanath, H. Bin Cho, J. H. Han, S. M. Kim, W. Bin Im, *J. Korean Ceram. Soc.* **2021**, *58*, 28–41.
[8] Z. Shen, S. Zhao, D. Song, Z. Xu, B. Qiao, P. Song, Q. Bai, J. Cao, G. Zhang, W. Swelm, *Small* **2020**, *16*, 1907089.
[9] F. Huo, W. Li, Y. Liu, X. Liu, C.-Y. Lee, W. Zhang, *J. Mater. Sci.* **2021**, *56*, 2814–2837.
[10] A. Ghaffarkhah, E. Hosseini, M. Kamkar, A. A. Sehat, S. Dordanihaghighi, A. Allahbakhsh, C. Kuur, M. Arjmand, *Small* **2022**, *18*, 2102683.
[11] N. Ma, S. O. Kelley, *Wiley Interdiscip. Rev. Nanomed. Nanobiotechnol.* **2013**, *5*, 86–95.
[12] I. J. Kramer, E. H. Sargent, *Chem. Rev.* **2014**, *114*, 863–882.
[13] P. Qiu, N. Zhou, H. Chen, C. Zhang, G. Gao, D. Cui, *Nanoscale* **2013**, *5*, 11512.
[14] J.-C. G. Bünzli, *Coord. Chem. Rev.* **2015**, *293–294*, 19–47.
[15] C. D. S. Brites, S. Balabhadra, L. D. Carlos, *Adv. Opt. Mater.* **2019**, *7*, 1801239.
[16] E. A. Mikhalyova, V. V. Pavlishchuk, *Theor. Exp. Chem.* **2019**, *55*, 293–315.
[17] E. Baranoff, J.-H. Yum, M. Graetzel, M. K. Nazeeruddin, *J. Organomet. Chem.* **2009**, *694*, 2661–2670.
[18] M.-H. Ho, B. Balaganesan, C. H. F. Chen, *Isr. J. Chem.* **2012**, *52*, 484–495.
[19] Y. Suzuri, T. Oshiyama, H. Ito, K. Hiyama, H. Kita, *Sci. Technol. Adv. Mater.* **2014**, *15*, 054202.
[20] G. Turkoglu, M. E. Cinar, T. Ozturk, *Molecules* **2017**, *22*, 1522.
[21] R. Braveenth, K. Y. Chai, *Materials* **2019**, *12*, 2646.
[22] Nonappa, *Beilstein J. Nanotechnol.* **2020**, *11*, 533–546.
[23] W. P. Lustig, J. Li, *Coord. Chem. Rev.* **2018**, *373*, 116–147.
[24] Y. Wu, W. Wu, *Adv. Opt. Mater.* **2021**, *9*, 2100281.
[25] J. C. G. Bünzli, K. L. Wong, *J. Rare Earth* **2018**, *36*, 1–41.
[26] K. L. Wong, J. C. G. Bünzli, P. A. Tanner, *J. Lumin.* **2020**, *224*, 117256.
[27] C. Würth, C. Lochmann, M. Spieles, J. Pauli, K. Hoffmann, T. Schüttrigkeit, T. Franzl, U. Resch-Genger, *Appl. Spectrosc.* **2010**, *64*, 733–741.
[28] N. I. Krimer, M. Mirenda, *Methods Appl. Fluoresc.* **2017**, *5*, 034001.
[29] K. Suzuki, A. Kobayashi, S. Kaneko, K. Takehira, T. Yoshihara, H. Ishida, Y. Shiina, S. Oishi, S. Tobita, *Phys. Chem. Chem. Phys.* **2009**, *11*, 9850.
[30] A. M. Brouwer, *Pure Appl. Chem.* **2011**, *83*, 2213–2228.
[31] L. Porrès, A. Holland, L.-O. Pålsson, A. P. Monkman, C. Kemp, A. Beeby, *J. Fluoresc.* **2006**, *16*, 267–273.
[32] D. Magde, R. Wong, P. G. Seybold, *Photochem. Photobiol.* **2002**, *75*, 327.
[33] P. C. Beaumont, D. G. Johnson, B. J. Parsons, *J. Chem. Soc. Faraday Trans.* **1998**, *94*, 195–199.
[34] S. Balabhadra, M. L. Debasu, C. D. S. Brites, R. A. S. Ferreira, L. D. Carlos, *J. Lumin.* **2017**, *189*, 64–70.
[35] R. Katoh, K. Suzuki, A. Furube, M. Kotani, K. Tokumaru, *J. Phys. Chem. C* **2009**, *113*, 2961–2965.
[36] H. Ishida, S. Tobita, Y. Hasegawa, R. Katoh, K. Nozaki, *Coord. Chem. Rev.* **2010**, *254*, 2449–2458.
[37] K. Binnemans, *Chem. Rev.* **2009**, *109*, 4283–4374.
[38] G. Bourhill, L. O. Pålsson, I. D. W. Samuel, I. C. Sage, I. D. H. Oswald, J. P. Duignan, *Chem. Phys. Lett.* **2001**, *336*, 234–241.
[39] E. Regalado-Pérez, N. R. Mathews, X. Mathew, *Sol. Energy* **2020**, *199*, 82–91.
[40] F. R. G. E. Silva, J. F. S. Menezes, G. B. Rocha, S. Alves, H. F. Brito, R. L. Longo, O. L. Malta, *J. Alloys Compd.* **2000**, *303–304*, 364–370.
[41] M. Fernandes, V. De Zea Bermudez, R. A. Sá Ferreira, L. D. Carlos, A. Charas, J. Morgado, M. M. Silva, M. J. Smith, *Chem. Mater.* **2007**, *19*, 3892–3901.
[42] E. A. Varaksina, M. A. Kiskin, K. A. Lyssenko, L. N. Puntus, V. M. Korshunov, G. S. Silva, R. O. Freire, I. V. Taydakov, *Phys. Chem. Chem. Phys.* **2021**, *23*, 25748–25760.
[43] B. L. An, K. W. Cheah, W. K. Wong, J. X. Shi, N. S. Xu, Y. S. Yang, M. L. Gong, *J. Alloys Compd.* **2003**, *352*, 143–147.
[44] C. Peng, H. Zhang, J. Yu, Q. Meng, L. Fu, H. Li, L. Sun, X. Guo, *J. Phys. Chem. B* **2005**, *109*, 15278–15287.
[45] X. Zhang, S. Wen, S. Hu, L. Zhang, L. Liu, *J. Rare Earth* **2010**, *28*, 333–339.
[46] L. N. Puntus, K. J. Schenk, J. G. Bünzli, *Eur. J. Inorg. Chem.* **2005**, *2005*, 4739–4744.
[47] L. R. Melby, N. J. Rose, E. Abramson, J. C. Caris, *J. Am. Chem. Soc.* **1964**, *86*, 5117–5125.
[48] J.-C. G. Bünzli, S. V. Eliseeva, *Basics of Lanthanide Photophysics in Lanthan. Lumin.* **2010**, 1–45.
[49] G. F. de Sá, F. R. G. E Silva, O. L. Malta, *J. Alloys Compd.* **1994**, *207–208*, 457–460.
[50] E. S. Andreiadis, R. Demadrille, D. Imbert, J. Pécaut, M. Mazzanti, *Chem. Eur. J.* **2009**, *15*, 9458–9476.
[51] A. E. Sedykh, R. Bissert, D. G. Kurth, K. Müller-Buschbaum, *Z. Kristallogr. - Cryst. Mater.* **2020**, *235*, 353–363.

[52] R. J. Batrice, J. A. Ridenour, R. L. Ayscue III, J. A. Bertke, K. E. Knope, *CrystEngComm* **2017**, *19*, 5300–5312.
[53] R. J. Batrice, R. L. Ayscue, A. K. Adcock, B. R. Sullivan, S. Y. Han, P. M. Piccoli, J. A. Bertke, K. E. Knope, *Chem. Eur. J.* **2018**, *24*, 5630–5636.
[54] R. L. Ayscue, C. P. Verwiel, J. A. Bertke, K. E. Knope, *Inorg. Chem.* **2020**, *59*, 7539–7552.
[55] A. E. Sedykh, S. A. Sotnik, D. G. Kurth, D. M. Volochnyuk, S. V. Kolotilov, K. Müller-Buschbaum, *Z. Anorg. Allg. Chem.* **2020**, *646*, 1710–1714.
[56] J. Wang, G. Hanan, *Synlett* **2005**, *2005*, 1251–1254.
[57] P. R. Matthes, J. Nitsch, A. Kuzmanoski, C. Feldmann, A. Steffen, T. B. Marder, K. Müller-Buschbaum, *Chem. Eur. J.* **2013**, *19*, 17369–17378.
[58] N. Dannenbauer, P. R. Matthes, T. P. Scheller, J. Nitsch, S. H. Zottnick, M. S. Gernert, A. Steffen, C. Lambert, K. Müller-Buschbaum, *Inorg. Chem.* **2016**, *55*, 7396–7406.
[59] N. Dannenbauer, P. R. Matthes, K. Müller-Buschbaum, *Dalton Trans.* **2016**, *45*, 6529–6540.
[60] S. Sato, M. Wada, *Bull. Chem. Soc. Jpn.* **1970**, *43*, 1955–1962.
[61] M. Latva, H. Takalo, V.-M. Mukkala, C. Matachescu, J. C. Rodríguez-Ubis, J. Kankare, *J. Lumin.* **1997**, *75*, 149–169.
[62] S. T. Frey, W. D. W. Horrocks, *Inorg. Chim. Acta* **1995**, *229*, 383–390.
[63] M. Latva, J. Kankare, *J. Coord. Chem.* **1998**, *43*, 121–142.
[64] N. Dalla-Favera, J. Hamacek, M. Borkovec, D. Jeannerat, F. Gumy, J. C. G. Bünzli, G. Ercolani, C. Piguet, *Chem. Eur. J.* **2008**, *14*, 2994–3005.
[65] K. Binnemans, *Coord. Chem. Rev.* **2015**, *295*, 1–45.
[66] X. Yang, C. Chan, D. Lam, D. Schipper, J. M. Stanley, X. Chen, R. A. Jones, B. J. Holliday, W.-K. Wong, S. Chen, et al., *Dalton Trans.* **2012**, *41*, 11449.
[67] K. P. Carter, K. E. Thomas, S. J. A. A. Pope, R. J. Holmberg, R. J. Butcher, M. Murugesu, C. L. Cahill, *Inorg. Chem.* **2016**, *55*, 6902–6915.
[68] J. A. Herder, B. W. Walusiak, C. L. Cahill, *J. Chem. Crystallogr.* **2021**, *51*, 317–336.
[69] X. Li, C.-Y. Wang, H.-M. Hu, *Inorg. Chem. Commun.* **2008**, *11*, 345–348.
[70] Y. Cha, X. Li, D. Ma, R. Huo, *Eur. J. Inorg. Chem.* **2014**, *2014*, 2969–2975.
[71] M. Hu, Y. Ling-Yu, F. Shao-Ming, *Mendeleev Commun.* **2016**, *26*, 304–306.
[72] K. Lunstroot, K. Driesen, P. Nockemann, L. Viau, P. H. Mutin, A. Vioux, K. Binnemans, *Phys. Chem. Chem. Phys.* **2010**, *12*, 1879–1885.
[73] M. Jakoby, C. Beil, P. Nazari, B. S. Richards, M. Seitz, A. Turshatov, I. A. Howard, *iScience* **2021**, *24*, 102207.
[74] E. Kreidt, L. Arrico, F. Zinna, L. Di Bari, M. Seitz, *Chem. Eur. J.* **2018**, *24*, 13556–13564.
[75] A. E. Kalugin, M. E. Minyaev, L. N. Puntus, I. V. Taydakov, E. A. Varaksina, K. A. Lyssenko, I. E. Nifant'ev, D. M. Roitershtein, *Molecules* **2020**, *25*, 3934.
[76] S. N. Melnikov, I. S. Evstifeev, S. A. Nikolaveskii, I. V. Ananyev, E. A. Varaksina, I. V. Taydakov, A. S. Goloveshkin, A. A. Sidorov, M. A. Kiskin, I. L. Eremenko, *New J. Chem.* **2021**, *45*, 13349–13359.
[77] *Apex 2 Suite*, BRUKER AXS Inc., Madison, WI, USA, **2014**.
[78] *XPREP (Version 2014/7), Program for Symmetry Analysis and Data Reduction of Diffraction Experiments*, Bruker AXS Inc., Madison, WI, USA, **2014**.
[79] G. M. Sheldrick, *Acta Crystallogr. Sect. C* **2015**, *71*, 3–8.
[80] G. M. Sheldrick, *Acta Crystallogr. Sect. A* **2008**, *64*, 112–122.
[81] C. B. Hübschle, G. M. Sheldrick, B. Dittrich, *J. Appl. Crystallogr.* **2011**, *44*, 1281–1284.
[82] A. A. Coelho, *J. Appl. Crystallogr.* **2018**, *51*, 210–218.

Manuscript received: September 2, 2022
Revised manuscript received: October 31, 2022
Accepted manuscript online: November 3, 2022
Version of record online: November 27, 2022